Journal of the European Ceramic Society 18 (1998) 1915–1921

PII: S0955-2219(98)00130-7
0955-2219/98/$—see front matter

Graceful Failure of Laminated Ceramic Tubes Produced by Electrophoretic Deposition

Luc J. Vandeperre* and Omer O. Van Der Biest

Departement Metaalkunde en Toegepaste Materiaalkunde, Katholieke Universiteit te Leuven, De Croylaan 2, 3001 Heverlee, Belgium

Abstract

The production of silicon carbide laminated ceramic tubes by electrophoretic deposition was investigated. Alternating deposition of SiC and graphite layers was obtained by depositing SiC from an acetone based suspension and by depositing the graphite interlayers from an iso-propyl alcohol based suspension. Laminated tubes were made and rings cut from these tubes were tested in diametral compression. Tough behaviour was observed: the SiC layers failed one by one and the cracks were deflected into the graphite interlayers. The failure event sequence is described and supported with simple linear elastic calculations for the expected load-displacement diagram. © 1998 Elsevier Science Limited. All rights reserved

Keywords: A. Shaping, B. Composites, C. Toughness, Toughening, D. SiC, electrophoretic deposition

1 Introduction

Ceramic laminates have been introduced as a simple way to obtain tough ceramic composites.[1] Laminates consist of layers of ceramic material in between which weak interlayers are introduced. These materials show a tough behaviour because when a crack propagates through a strong layer, it is deflected into the weak interlayer. As a result the other layers are not affected by this crack and can continue to carry load.

The processing techniques available today, however, allow only relatively simple shapes to be obtained. Taking into account possible applications for these materials such as tubes for heat exchangers and nozzles in chemical processing, it becomes apparent that there is a need for a process, which makes it possible to obtain ceramic laminates of complex shape at low cost. Electrophoretic deposition is investigated, therefore, as a production process for complex shaped ceramic laminates, since it has been shown that complex shapes can be obtained[2] and that this technique is very well suited to forming layered materials.[3] Moreover, electrophoretic deposition has been used also to infiltrate fibre preforms with a ceramic or glass-ceramic matrix.[4,5]

Electrophoretic deposition consists of applying an electric field to a suspension of a charged ceramic powder. In response to this electric field, the powder particles move (electrophoresis) and deposit at the electrode of opposite charge. Shaping is possible because the deposit takes the shape of the deposition electrode.

Earlier work included the development of a suspension for electrophoretic deposition of SiC,[6] the selection of a graphite suspension from which high quality graphite interlayers can be deposited, i.e. graphite interlayers which deflect cracks and have a satisfactory shear strength, and electrophoretic deposition of SiC/graphite laminated plates.[7] In this contribution the electrophoretic deposition of SiC/graphite laminated tubes is described, and the behaviour of rings cut from these tubes in diametral compression is investigated.

2 Experimental

The electrode set-up consisted of a hollow graphite cylinder as deposition electrode with a stainless steel rod situated in the centre as the counter electrode. (Fig. 1). Poly-tetrafluorethylene (PTFE) covers ensure a better electric field homogeneity. Further they provide support for the deposit during drying. The electrode set-up is attached to an in-house developed automated deposition cell which controls the residence time in the different

*To whom correspondence should be addressed.

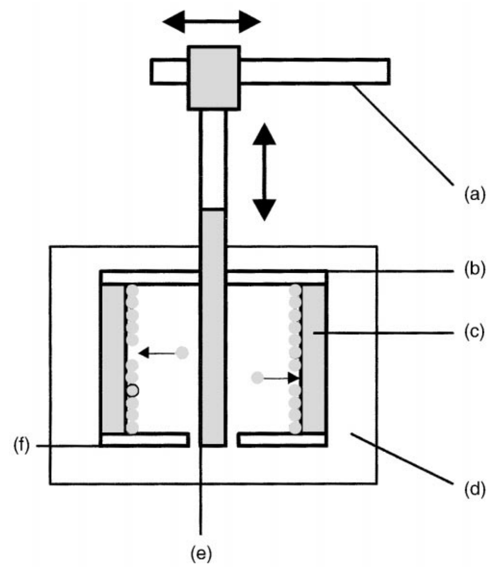

Fig. 1. Electrode set-up for electrophoretic deposition of tubes: (a) automated electrode positioner capable of moving the electrodes to one of four suspensions, (b) top PTFE cover, (c) graphite cylindrical deposition electrode, (d) suspension, (e) stainless steel rod serving as counter electrode, (f) bottom PTFE cover.

suspensions, and is able to move the electrodes from one suspension to another with a maximum of 4 suspensions. Deposition occurs on the inside of the graphite cylinder.

SiC layers are obtained by deposition from a suspension of a SiC powder (Superior Graphite, HSC-059s, $50\,g^{-1}$) in acetone with 5 vol% *n*-butylamine and 20 vol% iso-propyl alcohol. The iso-propyl alcohol is not required for deposition of SiC,[8] but is added to the acetonic suspension in order to match the drying rate of the SiC layers better to the drying rate of the graphite layers, which are deposited from a commercial colloidal graphite suspension (Superior Graphite, N°210) based on iso-propyl alcohol and diluted further with iso-propyl alcohol (70 vol%).

A laminated tube is obtained by consecutive deposition of SiC and graphite layers by applying 145 V so that the graphite deposition electrode is the positive electrode. After deposition of the required number of SiC and graphite layers, the deposit is dried and removed from the electrode. The tubes are sintered in a graphite furnace under vacuum at 2050°C for 30 min.

For evaluation of the layer thickness, the tubes are cut into a number of rings with equal width and the layer thickness is measured using an optical microscope (LOM).

For mechanical evaluation, these rings ($\varnothing_o$ $23 \times \varnothing_i\, 19 \times 5$ mm) are tested in diametral compression by placing the ring between two parallel horizontal plates which move towards each other while the resulting load is measured with a load cell.

3 Results and discussion

Figure 2 shows some examples of laminated tubes consisting of 19 SiC and 18 graphite layers produced by electrophoretic deposition.

3.1 Layer thickness

For the first tubes the deposition time was 2 min per SiC layer. Due to depletion of the suspension, the deposition rate drops and therefore, the thickness of the SiC layers decreases. The layer thickness data were used to construct a thickness master curve so that the deposition time per layer can be adapted in order to obtain layers of equal and preselected thickness. To test the master curve, the deposition times were calculated in order to obtain SiC layers of $100\,\mu m$. The actual average SiC layer thickness was $95 +/- 12\,\mu m$ (Fig. 3). The equation describing the master curve is:

$$T = T_0(1 - e^{-k.t}) \qquad (1)$$

where T is the cumulative SiC layer thickness, t is the cumulative deposition time from one suspension, whilst T_0 ($1500\,\mu m$) and k ($0{\cdot}121\ min^{-1}$) are fitting constants determined by fitting to experimental data. The thickness of the graphite layers was $10 +/- 3\,\mu m$.

3.2 Mechanical testing

Figure 4 shows the result of a mechanical test on a ring cut from a laminated tube, and Fig. 5 shows the sample after testing. The load-displacement

Fig. 2. Some examples of SiC/graphite laminated tubes consisting of 19 SiC layers ($95 +/- 12\,\mu m$) and 18 graphite layers ($10 +/- 3\,\mu m$). The outer diameter is 23 mm; the inner diameter is 19 mm and the length of the standing tube is 35 mm.

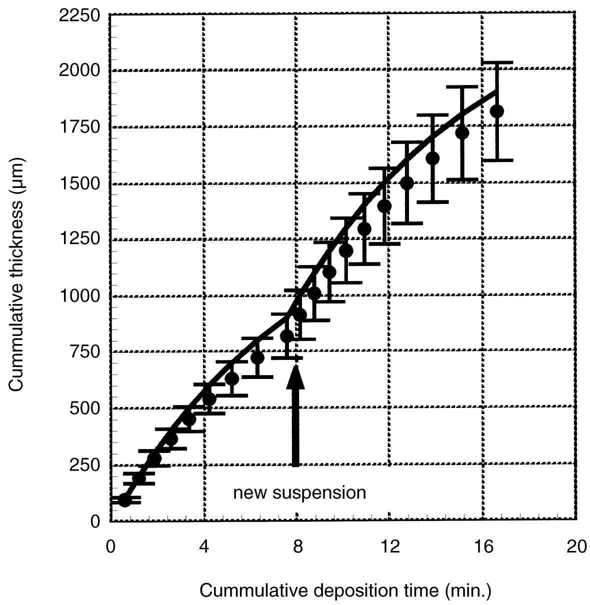

Fig. 3. Calculated (solid line) and experimental (dots) cumulative SiC layer thickness versus cumulative deposition time. After 9 SiC layers the SiC suspension was replaced by a new SiC suspension whilst the deposition experiment was continued.

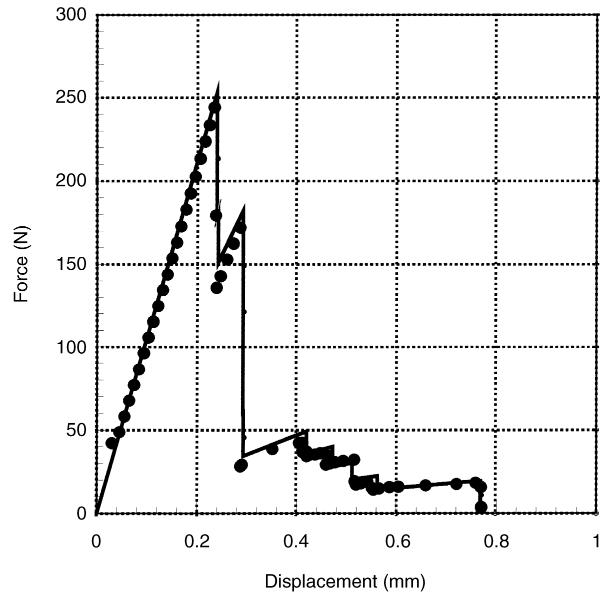

Fig. 4. Example of a load-displacement diagram recorded during a diametral compression test on a laminated ring (dots) and calculated overlay (solid line) showing that the slope changes due to failure can be reproduced accurately if the proposed failure mechanism is used for calculation.

diagram is of the saw-tooth type typical for laminates: as a SiC layer fails, the crack is deflected into the graphite interlayer. The rest of the ring can continue to carry load until all SiC layers have failed one by one. As a result the work to failure is increased and a graceful failure is obtained. The deflection of cracks at the graphite interlayers is very apparent in the photograph of a sample after failure.

Whilst rather complete descriptions of the behaviour of laminated ceramic plates in bending exist[9,10] as well as some predictions on their behaviour in tensile tests,[11] no description of the behaviour of laminated rings in diametral compression was found in literature. Based on visual damage observation during the test, stereoscopic investigation of the damage after the test, and by taking into account the stress distribution during loading of a ring (see below), a more complete description of the failure mechanism is proposed to consist of the following sequence of failure events (Fig. 6) : when the strength of the inner SiC layer is reached, it fails and the crack is deflected into the graphite interlayer. As a result one obtains a thinner ring and two thin C-rings inside this ring which are still retained by the outer layers. As the strength of the next inner layer of the full ring is reached, again that layer fails and the crack is deflected in the next graphite interlayer, resulting in the formation of a new pair of thin C-rings. Finally the ring will have been transformed completely in a series of thin C-shaped layers, which will then fail layer by layer. The latter because the horizontal plates also retain the C-rings so that they can still carry load.

The relations between the displacement, applied force and stress can be derived by combining the solution for an O-ring and a C-ring. The maximum tensile stress in an O-ring is related to the applied force by:[12]

$$\sigma_{\theta\theta} = -\frac{F}{S}\left(\frac{1}{\pi}\,\frac{r_0^2}{r_0^2+h^2} + \frac{r_0^2}{2h^2}\,\frac{y}{y+r_0} \times \left[\frac{2}{\pi}\,\frac{r_0^2}{r_0^2+h^2} - \cos\theta\right]\right) \qquad (2)$$

with :
r_2: the outer radius of the ring (mm);
r_1: the inner radius of the ring (mm);
r_0: the average radius of the ring (mm) ($=(r_1+r_2)/2$);
y: the distance from the average radius (mm) ($=r-r_o$);
S: the surface area of the ring (mm^2) ($=(r_2-r_1).t$);
t: the thickness of the ring (mm);
$\sigma_{\theta\theta}$: the stress in the θ direction (MPa, see Fig. 7) and

$$h^2 = \frac{1}{S}\int \frac{r_0.y^2}{r_0+y}\,dS = \frac{r_0^2}{(r_2-r_1)}\ln\left(\frac{r_2}{r_1}\right) - r_0^2 \qquad (3)$$

The displacement is related to the force through:[7]

$$d = \frac{2.F.r_0}{E.S}\,\frac{r_0^2}{h^2}\left(\frac{\pi}{8}\frac{1}{\pi}\,\frac{r_0^2}{r_0^2+h^2}\right) \qquad (4)$$

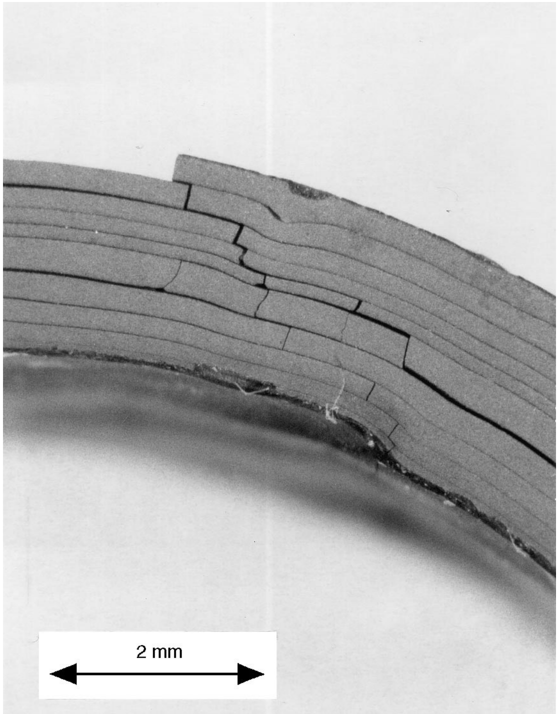

Fig. 5. Detail of a ring after testing showing the occurrence of crack deflection into the graphite interlayers

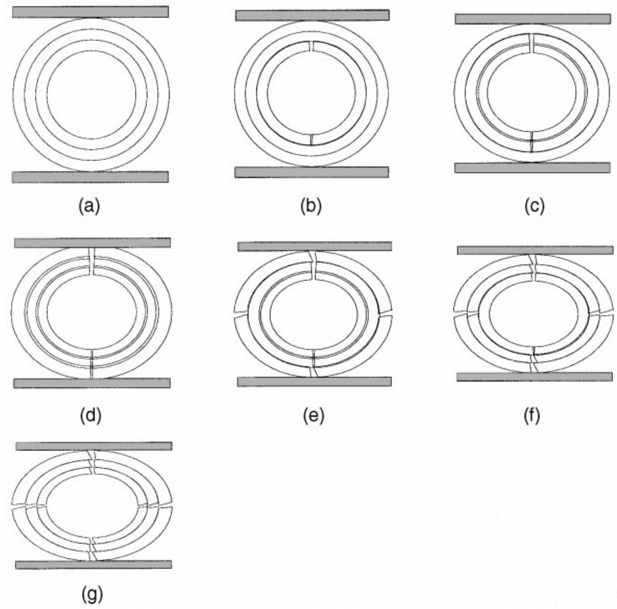

Fig. 6. Failure sequence in a laminated ring in diametral compression for an infinite Weibull modulus: (a) elastic loading of the ring, (b) the strength is reached and the most inner layer fails. The crack is deflected in the graphite interlayer, resulting in the formation of 2 C-rings of 1 layer thickness, (c) the next layer fails, (d) the last layer fails, (e) the strength of the outer C-ring is reached, (f) the next C-ring fails, (g) the last C-ring fails.

with :
E: Young's modulus (MPa);
d: displacement of the loading plate (mm).

For a C-ring these relations can be derived from the exact solution for a C-ring under end shear loading: the effect of a concentrated force is only important close to the point where the concentrated force acts on a body (St. Venants principle). The solution for the stresses is:

$$\sigma_{rr} = \frac{F}{Rt}\left(\frac{(-r_1^2 + r_2^2)}{r} + r + \frac{r_1^2 r_2^2}{r^3}\right)\sin\theta \qquad (5a)$$

$$\sigma_{\theta\theta} = \frac{F}{Rt}\left(\frac{-(r_1^2 + r_2^2)}{r} + 3r - \frac{r_1^2 r_2^2}{r^3}\right)\sin\theta \qquad (5b)$$

$$\sigma_{r\theta} = \frac{F}{Rt}\left(\frac{(-r_1^2 + r_2^2)}{r} + r + \frac{r_1^2 r_2^2}{r^3}\cos\theta\right. \qquad (5c)$$

with :

$$R = (r_1^2 - r_2^2) + (r_1^2 + r_2^2)\ln\left(\frac{r_2}{r_1}\right) \qquad (6)$$

In order to obtain the resulting displacement, we used the definitions of the strain:

$$e_{rr} = \frac{1}{E}(\sigma_{rr} - \nu\sigma_{\theta\theta}) \qquad (7a)$$

$$e_{\theta\theta} = \frac{1}{E}(\sigma_{\theta\theta} - \nu\sigma_{rr}) \qquad (7b)$$

$$e_{r\sigma} = \frac{\sigma_{r\theta}}{G} \qquad (7c)$$

and the relation between the strain and the displacements:

$$e_{rr} = \frac{\partial u_r}{\partial r} \qquad (8a)$$

$$e_{\theta\theta} = \frac{u_r}{r} + \frac{1}{r}\frac{\partial u_\theta}{\partial \theta} \qquad (8b)$$

$$e_{r\theta} = \frac{\partial u_\theta}{\partial r} + \frac{1}{r}\frac{\partial u_r}{\partial \theta} - \frac{u_\theta}{r} \qquad (8c)$$

Explication of the expressions for the stress [eqn (5) in eqn (7)], followed by substitution of this result in eqn (8) and partial integration leads to the following expression for the displacement in the direction of the radius, u_r, and in the direction of the circumference, u_θ:

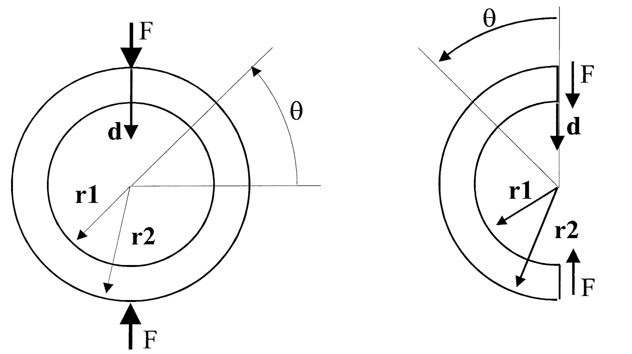

Fig. 7. Conventions for the calculation of the stresses and displacements in O- and C-rings.

$$u_r = \frac{\sin\theta}{E}\left(A(1-\nu)\ln r + Br^2(1-3\nu) + \frac{c}{r^2}(1-\nu)\right) - \frac{2A}{E}(\sin\theta + \theta\cos\theta) \quad (9a)$$

$$u_\theta = -\frac{\cos\theta}{E}\left(A(1-\nu) - A(1-\nu)\ln r + Br^2(5+\nu) + \frac{C}{r^2}(1+\nu)\right) + \frac{2A}{E}\theta\sin\theta \quad (9b)$$

with :

$$A = \frac{-F(r_1^2 + r_2^2)}{Rt} \quad (10)$$

$$B = \frac{-A}{2(r_1^2 + r_2^2)} \quad (11)$$

$$C = \frac{Ar_1^2 r_2^2}{2(r_1^2 + r_2^2)} \quad (12)$$

as a result the relation between displacement and force is (displacement in the r-direction for $\theta = \pi$):

$$d = \frac{2\pi}{E}F\frac{(r_1^2 + r_2^2)}{Rt} \quad (13)$$

Using the above relations, simulations of load-displacement diagrams for laminated rings in diametral compression can be made. A computer program was written which assembles the ring as a number of layers. In order to define the geometry of the ring, the inner diameter is stored in a database together with the strength and the thickness of each layer. If an equal strength value is given to all layers, this simulates a material with an infinite Weibull modulus. In order to simulate a material with a finite Weibull modulus, a random strength value is taken from the Weibull distribution for each layer. As the graphite interlayers prevent cracks from growing from one layer to another, each layer will indeed only fail when its strength is reached.

In order to predict what the next failure event will be, the program calculates for all layers what the total displacement of the loading plate should be in order to reach a maximum stress within that layer equal to the strength of that layer. The layer showing the lowest displacement required to reaching a stress equal to its strength, is taken as the next layer which fails. Note that the first layer to fail is not necessarily the layer with the lowest strength, since also the position of the layer and the stress distribution in the ring has to be taken into account.

Initially, when the ring is intact, the graphite interlayers are assumed to be capable of perfect load-transfer so that the stress can be evaluated as if it were a monolithic ring. The maximum stress in each layer of the intact ring as a function of the displacement can be evaluated by using eqns (2) and (4), where y is varied as a function of the position of each layer within the ring.

Normally it is expected that the inner ring will fail first, as the stress is at maximum in this layer. Upon failure of the inner layer, the deflection of the crack into the interlayer, is simulated by removing the inner layer from the ring, and replacing this layer by two thin C-rings clamped within the now thinner O-ring. Further, it is assumed, that once a crack has been deflected in a graphite interlayer, the graphite interlayer is no longer capable of load transfer. Hence the force required to deform the now thinner O-ring together with the newly created C-rings can be found by superposition of the force required to deform each of these components independently. During further calculations the program will now evaluate for each layer in the O-ring and for each of these newly created C-rings, what the required displacement is in order to reach the strength of that layer in the O-ring or the strength of each of the C-rings.

If instead of the inner layer, a layer in the centre of the ring fails, e.g. because it has a very low strength, this layer is removed from the ring. However, as no load transfer is assumed to occur by graphite interlayers in which a crack has been deflected, this results in the creation of two O-rings: one consisting of all layers from the outer layer until the layer next to the failing layer, and one consisting of all layers starting with the layer one further than the failing layer until the most inner layer. Further the failed layer is replaced by two C-rings in between these O-rings.

The force required for deformation of this configuration, is obtained by superposition of the force required to deform each of the O-rings and each of the C-rings. After failure of a C-ring, it is assumed that no more load is taken by that part of the ring.

Figure 8 shows some examples for laminated rings having an internal radius of 9.5 mm and an average strength of 430 MPa. The average strength of 430 MPa was selected since the strength of the electrophoretically deposited SiC was found to be 430 MPa with a Weibull modulus of 3.7.[13]

If all layers have an equal strength, the failure sequence will be as in Fig. 6: first the O-ring will fail layer by layer starting from the inner layer, followed by the failure of the so created C-rings starting from the outside.

Apart from simulations, the above program can also be used to evaluate whether the stiffness decrease observed during real tests is in accordance with what is expected based on the above failure mechanism. Since the strength values of the layers are not known *a priori*, the displacements at which failure of a layer occurs are taken from the measured load-displacement diagram. Further the apparent Young's Modulus is evaluated from the initial slope of the curve. The slope changes in the load displacement diagram due to failure of the layers are then calculated. In Fig. 4 a calculated overlay on an experimental result is shown: the changes in the stiffness observed during the test can indeed be reproduced if the load-displacement diagram is calculated following the proposed failure events sequence. It should be noted that sometimes more layers do fail together in real materials since not all layers have an equal strength.

4 Conclusions

Electrophoretic forming of composite ceramic laminated tubes is possible: SiC/graphite laminated tubes can be obtained and the layer thickness can be controlled easily.

Moreover, rings cut from such tubes show graceful failure: cracks are deflected at the graphite interlayers, resulting in an increase of the work to failure.

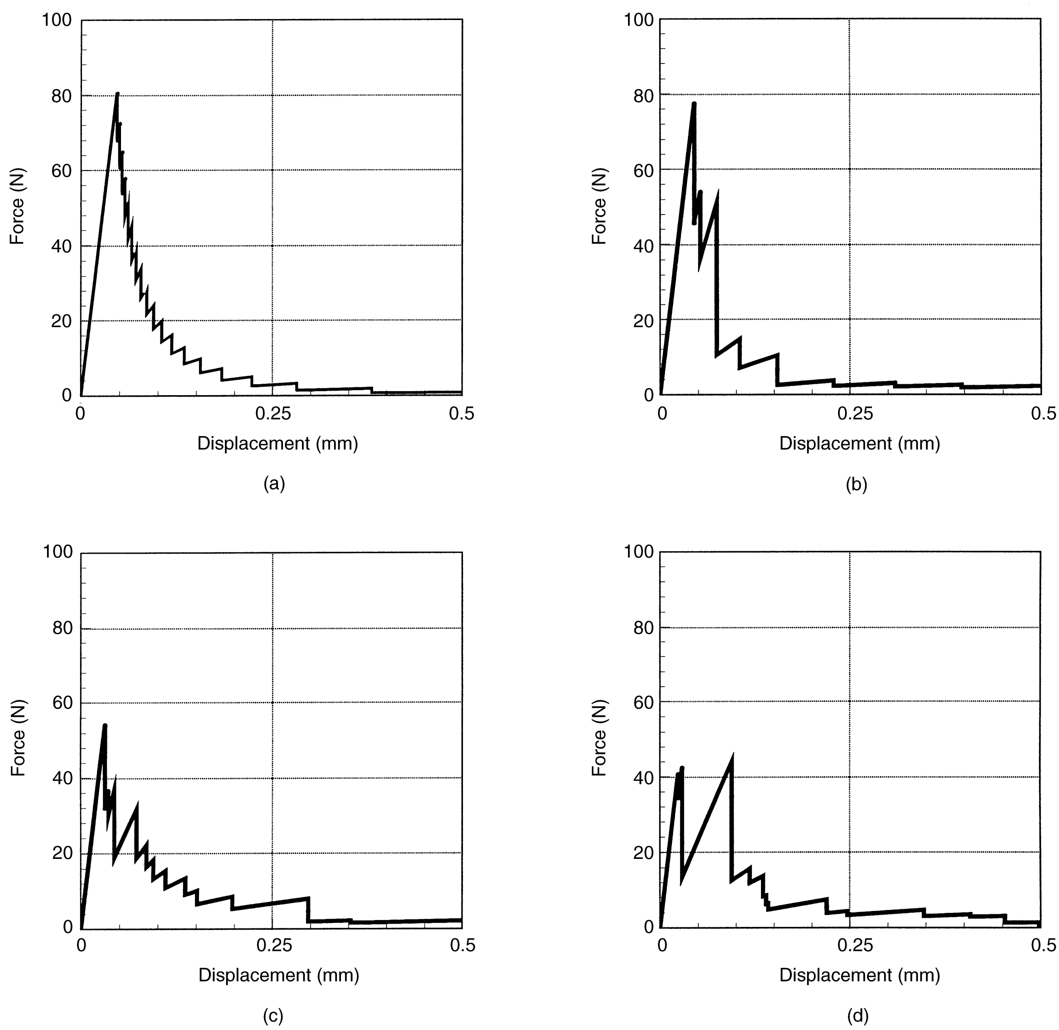

Fig. 8. Partial calculated load-displacement diagrams (up to 0·5 mm displacement) for a laminated ring of unit thickness consisting of 20 SiC layers of 100 μm, with a Young's modulus of 450 GPa and an inner diameter of the ring of 9·5 mm for (a) an average strength of 430 MPa and an infinite Weibull modulus, (b,c & d) examples for an average strength of 430 MPa and a Weibull modulus of 3·7.

The sequence of failure events during diametral compression consist of a layer by layer failure of the ring resulting in the formation of individual C-rings of one layer thickness followed by the failure of these C-rings. A very good agreement between simulated and measured load-displacement diagrams was obtained using a simple linear elastic calculation, under the assumption that once a crack has been deflected into a graphite interlayer, de-bonding occurs to such an extent that the interlayer can no longer transfer load between the SiC layers. The force to deform the specimen is obtained by superposition of the force required to deform each of the de-bonded parts.

Acknowledgements

This work was supported by the Brite-Euram programme of the Commission of the European Communities under Project BE-7414/BRE2-0564.

References

1. Clegg, W. J., Kendall, K., Alford, N., Button, T. W. and Birchall, J.D., A simple way to make tough ceramics. *Nature*, 1990, **347**, 455–457.
2. Kennedy, J. H. and Foissy, A., Fabrication of beta-alumina tubes by electrophoretic deposition from suspensions in dichloromethane. *J. Electrochem. Soc.*, 1975, **122**, 482–486.
3. Sarkar, P., Huang, X. and Nicholson, P. S., Structural ceramic microlaminates by electrophoretic deposition. *J. Am. Ceram. Soc*, 1992, **75**(10), 2907–2909.
4. Kooner, S., Fibre reinforced ceramic matrix composite fabrication by electrophoretic infiltration. *The Materials Challenge News Bulletin*, 1995, **8**, 27–29.
5. Boccaccini, A. R., Trusty, P. A., Taplin, D. M. R. and Ponton, C. B., Colloidal processing of a mullite martrix material suitable for infiltrating woven fibre preforms using electrophoretic deposition. *J. Eur. Ceram. Soc*, 1996, **16**, 1319–1327.
6. Vandeperre, L., Van Der Biest, O., Bouyer, F., Persello, J. and Foissy, A., Electrophoretic forming of silicon carbide ceramics. *J. Eur. Ceram. Soc*, 1997, **17**(2), 373–376.
7. Vandeperre, L., Van Der Biest, O. and Clegg, W. J., Silicon carbide laminates with carbon interlayers by electrophoretic deposition. *Key Engineering Materials*, Vols 127–131, Trans Tech. Publications, Switzerland, 1997, pp.567–574.
8. Vandeperre, L. and Van Der Biest, O., Influence of isopropyl alcohol addition on the electrophoretic deposition of SiC from acetone with n-butylamine. *Key Engineering Materials*, Vols 132–136, Trans Tech. Publications, Switzerland, 1997, pp. 293–296.
9. Phillips, A. J., Clegg, W. J. and Clyne, T. W., Fracture behaviour of ceramic laminates in bending: I. Modelling of crack propagation, *Acta Metall. Mater.*, 1993, **41**(3), 805–817.
10. Folsom, C. A., Zok, F. W. and Lange, F. F., Flexural properties of brittle multilayer materials: I, Modeling. *Journal of the American Ceramic Society*, 1994, **77**(3), 689–696.
11. Clegg, W. J., Phillips, A. J. and Clyne, T. W., The failure of layered ceramics in bending and tension, composites, 1994, **25**(7), 254–233.
12. Ford, H., Advanced mechanics of materials, Longman, Green and Co. Ltd.,London, 1969, pp. 254–269.
13. Vandeperre, L., Bouyer, F., Foissy, A. and Van Der Biest, O., Silicon Carbide/Graphite Laminates Shaped by Electrophoretic Deposition, submitted to the *Bulletin of the American Ceramic Society*.